Automotive Experiences
Vol. 8 No. 2 (2025) pp. 281-295
p-ISSN: 2615-6202 e-ISSN: 2615-6636

Research Paper

Enhancing Stoichiometric Methane-Air Flames: The Role of N_2O Replacement

Aris Purwanto[1], **Herman Saputro**[2], **Akhmad Faruq Alhikami**[3], **Fudhail Abdul Munir**[4]

[1]Department of Mechanical Engineering, Universitas Negeri Surabaya, 60231, Surabaya, Indonesia
[2]Department of Mechanical Engineering Education, Universitas Sebelas Maret, 57161, Surakarta, Indonesia
[3]Department of Mechanical Engineering, Universitas Islam Malang, 65145, Malang, Indonesia
[4]Faculty of Mechanical Engineering, Universiti Teknologi PETRONAS, 31000, Perak, Malaysia

arispurwanto@unesa.ac.id

https://doi.org/10.31603/ae.13422

Published by Automotive Laboratory of Universitas Muhammadiyah Magelang

Article Info
Submitted: 19/04/2025
Revised: 31/08/2025
Accepted: 02/09/2025
Online first: 02/09/2025

Abstract

The oxidizer is used in aviation propellants for its relatively high impulse density and non-toxic nature. At elevated temperatures, nitrous oxide (N_2O) decomposes into approximately 33% oxygen (O_2) and 67% nitrogen (N_2), providing a higher oxygen content than ambient air. This decomposition enables N_2O to produce higher flame temperatures than air. Previous studies have shown that N_2O addition improves flame stability in methane combustion systems. This study examined the substitution of O_2 with N_2O in stoichiometric methane–air premixed flames, using both numerical and experimental methods. One-dimensional and two-dimensional simulations with CHEMKIN PRO revealed that replacing air with N_2O increases flame temperature but reduces laminar flame speed, mainly due to lower local oxygen concentrations in the reaction zone. The simulations also showed that nitrogen oxides (NO_x) emissions increase significantly in the post-reaction zone, while carbon monoxide (CO) and carbon dioxide (CO_2) emissions decrease. Experimental results confirmed that controlled N_2O addition enhances flame stability, but excessive concentrations can trigger combustion instabilities. Overall, the findings indicate that introducing up to 20% N_2O can increase flame temperature and reduce CO emissions in methane flames.

Keywords: Nitrous Oxide; Methane-air flame; Flame stability; NOx emission; flame speed

1. Introduction

The development of propellants in the aviation industry is one of the most crucial areas to research [1]. Conventional propellants such as hydrazine and cryogenic propellants have long been favored for their high energy density and consistent performance [2], [3], [4]. However, those propellant has some issues like toxicity, costly handling and storage, and complex cryogenic infrastructure [5], [6], [7]. These issues lead to the development of green propellant which uses non-toxic fuel [8], [9]. NOFBX (Nitrous Oxide Fuel Blend) is a next-generation propellant designed to replace conventional rocket fuels that are costly, toxic, and require cryogenic infrastructure [10], [11]. As a medium-pressure liquid oxidizer, NOFBX can be produced, stored, and distributed more efficiently, eliminating the need for specialized facilities. These properties have the potential to lower launch operational costs, decrease hazardous waste management expenses, and shorten mission preparation times [7]. Besides that, the advantage of N_2O as one of the alternatives as an oxidizer in propellants for aviation, N_2O has a relatively high impulse density, and it is also non-toxic [12], [13], [14]. At high temperatures, N_2O can decompose into 33% O_2 and 67% N_2, and this decomposition results in a higher oxygen content compared to air [15]. This oxygen-rich condition can improve combustion efficiency [16]. However, combustion using N_2O can produce significantly higher NOx emissions

compared to air [17], which can degrade the ozone layer in the atmosphere. Therefore, the addition of N_2O in hydrocarbon fuels is important to study in order to understand the relationship between combustion efficiency and exhaust gas emissions.

Several studies related to the addition of N_2O as an oxidizer have been widely conducted by researchers around the world [18], [19], [20], [21], [22]. A study by Wang [18] showed that the use of N_2O in NH_3-N_2O mixtures resulted in a higher laminar burning velocity compared to NH_3-air mixtures. Another study by Wang [23] demonstrated that N_2O can increase the pressure during hydrogen combustion in a closed vessel. In addition to enhancing laminar burning velocity and increasing pressure, the use of N_2O as an oxidizer can also reduce carbon emissions, including CO and CO_2 [24], [25], [26], [27]. A simulation study by Chen [17] showed that NOx production could be reduced under highly fuel-rich conditions. A study by Harada [27] also indicated that NOx emissions could be reduced when using NH_3 as the fuel. A study by Choy [28] showed that flames with impinging IDFs (Impinging Diffusion Flames) produce higher NOx emissions and noise radiation compared to open IDFs, possibly due to the absence of NO reburning. The closer the impingement plate is to the burner, the higher the noise levels. A study by Shih and Hsu [29] demonstrated that NO formation strongly depends on flame temperature, H_2 content, pressure, and the type of dilution gas, with thermal routes being dominant at high temperatures and N_2O or NNH routes dominant at low H_2 content or low pressure. Besides that, N2O mixed with hydrocarbon fuel can enhance the ignition delay [30], [31], and flame extinction limit [32].

The combustion of methane (CH_4) with N_2O has also been widely studied, as N_2O can increase the temperature and combustion velocity. Some studies related to CH_4-N_2O mixtures indicate that N_2O can enhance the burning velocity. Razus [33] showed that CH_4-N_2O combustion results in a high burning velocity. Additionally, Razus' study found that adding N_2 to CH_4-N_2O mixtures leads to a decrease in burning velocity. Moreover, CH_4 combustion in an oxygen-rich environment can increase the reactivity of the methane flame and NO formation. Thus, in oxygen-rich environments, whether from decomposed N_2O or an oxygen-rich mixture, the reactivity of the methane flame increases. In this study, we aim to investigate the effect of replacing N_2O on the composition of N_2 and O_2 in stoichiometric methane-air flames. We employ a simulation approach using CHEMKIN Pro and Fluent, and also conduct experiments to examine the impact of N_2O replacement on flame stability in methane combustion.

2. Methods

A one-dimensional numerical simulation was carried out using the CHEMKIN PRO software package [34], specifically employing the PREMIXED module to model the laminar premixed flame [35]. This module is designed to solve the governing equations for mass, momentum, energy, and species conservation in a steady, one-dimensional domain, which is ideal for investigating fundamental flame characteristics under controlled conditions [36]. The simulation provided detailed profiles of key parameters along the axial direction of the flame, including temperature, velocity, pressure, and species concentrations, these results provide a validated kinetic baseline that serves as a reference. Additionally, it facilitated the analysis of reaction pathways by calculating reaction rates, species production and consumption rates, and the net heat release rate, all of which are crucial for understanding the flame structure and combustion behavior. In this study, the GRI-Mech 3.0 reaction mechanism was employed due to its comprehensive and validated set of elementary reactions specifically optimized for methane and natural gas combustion [37]. This mechanism includes detailed chemistry of hydrocarbon oxidation, nitrogen species, and pollutant formation, making it suitable for accurately capturing the chemical kinetics involved in methane-air combustion, particularly when exploring the effects of additives such as nitrous oxide (N_2O) [38], [39], [40].

To achieve stable and accurate numerical solutions, adaptive meshing was applied throughout the simulation. The mesh refinement was governed by two key parameters: the gradient-based control (GRAD) and the curvature-based control (CURV), both set at a sensitivity value of 0.1. The maximum number of

grid points (NTOT) permitted in the domain was limited to 1000, with 20 initial adaptive points introduced to improve resolution where needed. Simulations were conducted by incorporating both thermal diffusion effects and multicomponent species transport, ensuring detailed modeling of the flame dynamics. A mesh independence study was also performed by comparing the temperature profiles obtained using two different NTOT values 1000 and 15,000. The comparison revealed only minor discrepancies between the results, indicating that the solution was not significantly affected by further mesh refinement. As such, the simulation results were confirmed to be grid-independent, demonstrating robustness concerning spatial discretization.

In this study, a methane–air–N_2O mixture was employed to investigate the influence of varying N_2O concentrations on the behavior of premixed methane-air flames. The numerical simulations were conducted under ambient conditions, with an initial temperature of 300 K and a pressure of 1 atm. In this study, in addition to one-dimensional simulations, two-dimensional Computational Fluid Dynamics (CFD) simulations were conducted to capture the spatial distribution of flow and reactive species, CFD software was widely used for the combustion phenomena [41], [42], [43], [44]. In this study, to reduce computational cost, a two-dimensional configuration was employed. The ANSYS Fluent software was used for numerical simulations to investigate the flame configuration and spatial distribution of temperature and species within the burner geometry. The simulations were performed on an Intel Core i7 computer with 16 GB of RAM. The SIMPLE algorithm with pressure-based solver was used in this simulation, The governing equations consist of the steady-state, two-dimensional Navier–Stokes equations, along with conservation equations for mass, energy, and species transport for all participating chemical species [45]. This simulation also operated under the following assumptions: (1) steady-state combustion, (2) Dufour and Soret effects neglected, (3) gas radiation neglected, (4) laminar flow, and (5) incompressible flow with ideal gas conditions. Based on all these assumptions, the conservation equations are formulated in Eq. (1) to Eq. (5).

Continuity Conservation:

$$\frac{\partial(\rho u)}{\partial x}+\frac{\partial(\rho v)}{\partial r}+\frac{\rho v}{r}=0 \tag{1}$$

Momentum Equations
Axial Direction

$$\rho u\frac{\partial u}{\partial x}+\rho v\frac{\partial u}{\partial r}=-\frac{\partial p}{\partial x}+\mu\left(\frac{\partial^2 u}{\partial x^2}+\frac{\left(\frac{1}{r}\right)\partial}{\partial r}\left(r\frac{\partial u}{\partial r}\right)\right) \tag{2}$$

Radial Direction

$$\rho u\frac{\partial v}{\partial x}+\rho v\frac{\partial v}{\partial r}=-\frac{\partial p}{\partial r}+\mu\left(\frac{\partial^2 v}{\partial x^2}+\frac{\left(\frac{1}{r}\right)\partial}{\partial r}\left(r\frac{\partial v}{\partial r}\right)-\frac{v}{r^2}\right) \tag{3}$$

Energy Equation

$$\rho u\frac{\partial h}{\partial x}+\rho v\frac{\partial h}{\partial r}=\nabla\cdot(k\nabla T)+\Sigma\, h_i\,\dot{\omega}_i \tag{4}$$

Species Transport Equation

$$\rho u\frac{\partial Y_i}{\partial x}+\rho v\frac{\partial Y_i}{\partial r}=\nabla\cdot(\rho D_i\nabla Y_i)+\dot{\omega}_i \tag{5}$$

The detailed computational model is shown in **Figure 1**. An open-domain computational setup was utilized to simulate the flame behavior under varying conditions. Given the symmetrical nature of the flame, only half of the domain was modeled in order to optimize computational resources and reduce simulation time without compromising accuracy. Methane (CH_4) was selected as the fuel, while the oxidizer was modeled as atmospheric air, consisting of 21% oxygen (O_2) and 79% nitrogen (N_2) by volume. To investigate the effect of nitrous oxide (N_2O) addition, a portion of the air was systematically replaced with N_2O, with replacement levels ranging from 5% to 20% by volume. The boundary conditions at the inlet were defined as a uniform velocity inlet with a flow speed of 0.8 m/s. The outlet was set as a pressure outlet to allow for natural pressure-driven flow. The inlet and backflow temperatures were maintained at 295 K to simulate ambient conditions. The wall boundaries were specified with a no-slip condition, ensuring zero velocity at the wall surfaces to represent viscous effects near solid boundaries accurately.

In this simulation, a tetrahedral mesh was employed to discretize the computational domain [46]. A mesh refinement was applied, particularly around the wall regions near the reaction zone, to accurately capture steep gradients in temperature and species concentration. To ensure the reliability of the numerical results, a grid indepen-

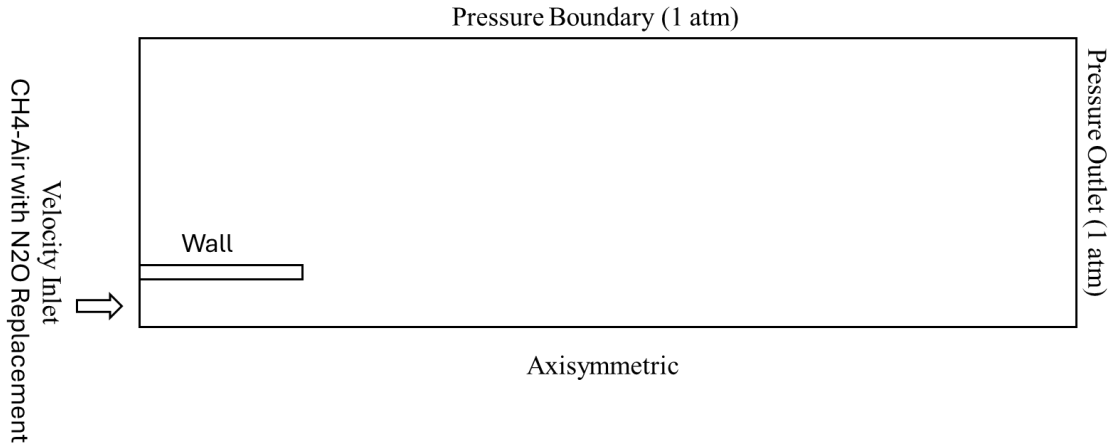

Figure 1. Computational domain

dence test was conducted by varying the refinement mesh sizes. Among the tested configurations, a refinement size of 0.2 mm yielded the most stable results, with a deviation of less than 1.8% compared to finer meshes [47], [48]. The simulations were considered converged when the residuals of the governing equations dropped below 10^{-5}. This convergence criterion ensures that the iterative solution process has reached a sufficiently accurate solution where further iterations result in negligible changes.

To validate the simulation results, we conducted a combustion experiment of CH_4-Air premixed flame with the N_2O replacement. In this experiment, we used a coaxial Bunsen burner with an inner diameter of 11.5 mm and an outer diameter of 14 mm. The burner is equipped with a honeycomb to help stabilize the gas flow toward the burner outlet. Additionally, the burner nozzle is designed with a concentric reducer to ensure the flow remains laminar. Each gas was controlled using digital mass flow meter Brooks 5850E (Brooks Instrument, USA), A B-type thermocouple, capable of measuring temperatures up to approximately 2000 K, was used. The thermocouple outputs were recorded and translated into temperature data using a data logger (NI-USB-TC01, National Instruments Corp., USA). The research scheme was shown in **Figure 2**. The details of the mole fraction for the chemical reaction for each case in stoichiometric conditions are shown in **Table 1**. We started the experiment by changing the concentration of N_2O at 0, 5, 10, 15, 20, and 25% in order to perform the methane–air flame test. The research was restricted to 20% N_2O addition, though, because the flame became unstable at 25%.

For the temperature measurement we corrected the measurement data with thermal radiation which proposed by Yunus and Rabee [49], [50] the equation shown in Eq. (6).

$$T = T_{TC} + \frac{\varepsilon \sigma d_{TC} (T_{TC}^4 - T_{surr}^4)}{kNu} \quad (6)$$

where, T_{tc} is thermocouple temperature (k), ε is thermocouple bead emission, σ is Stefan–Boltzmann constant (5.67×10^{-8}W/m^{2}K^4), d_{tc} is thermocouple bead diameter (m), T_{surr} is surrounding temperature (k), k is thermal conductivity of hot gases (W/mK), Nu is Nusslet number.

3. Results and Discussion

3.1. Numerical Simulation

An EQUIL code was used to conduct the numerical simulation of adiabatic flame temperature of CH_4-air with N_2O replacement, in this study we conducted N_2O replacement from 0 to 20% in stoichiometric CH_4-air flame. Based on the simulation results presented in the **Figure 3**,

Table 1. Mole fraction for each simulation case

Species	0% N_2O	5% N_2O	10% N_2O	15% N_2O	20% N_2O
CH_4	0.0950	0.0950	0.0950	0.0950	0.0950
O_2	0.1900	0.1806	0.1711	0.1616	0.1521
N_2	0.7149	0.6792	0.6434	0.6077	0.5719
N_2O	0	0.0452	0.0905	0.1357	0.1810

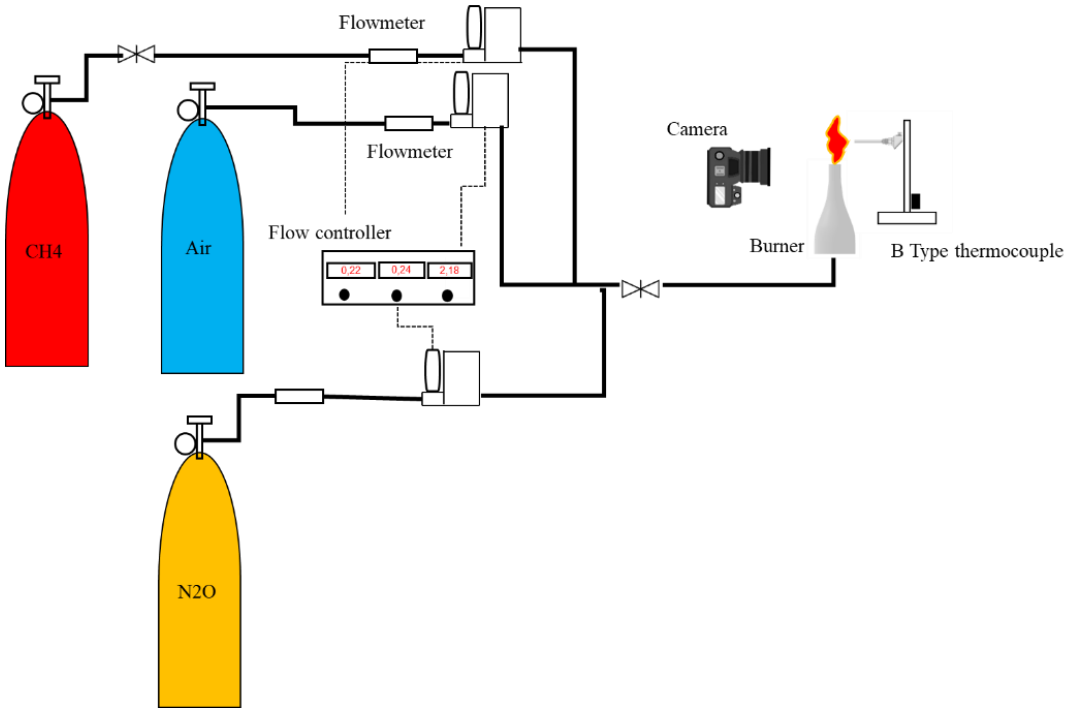

Figure 2. Experimental setup

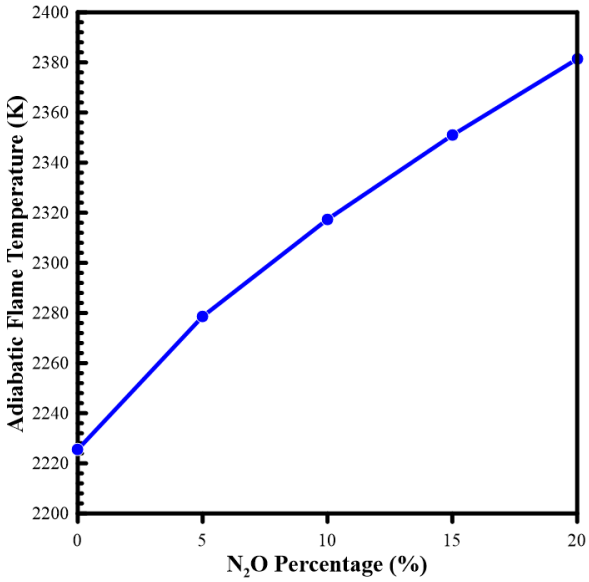

Figure 3. Adiabatic flame temperature of different N_2O concentration

the addition of nitrous oxide (N_2O) to a stoichiometric methane-air premixed flame has a noticeable impact on the adiabatic flame temperature. The baseline temperature of a stoichiometric CH_4-air flame without any N_2O addition is approximately 2230 K. As N_2O is introduced into the mixture, a consistent increase in flame temperature is observed, indicating enhanced combustion intensity.

When 5% N_2O is added to the reactant mixture, the adiabatic flame temperature rises to 2280 K. This trend continues with further N_2O enrichment: at 10% N_2O, the flame temperature increases to 2320 K; at 15%, it reaches 2360 K; and finally, with a 20% addition of N_2O, the temperature peaks at 2380 K. This progressive rise in flame temperature suggests that N_2O acts as an effective oxidizing agent, contributing additional oxygen and thermal energy through its decomposition, which enhances the overall combustion process.

Following the analysis of the adiabatic flame temperature, a series of simulations were conducted to investigate the effect of N_2O addition on the laminar flame speed of stoichiometric CH_4-air premixed flames. In this study, the PREMIX module of CHEMKIN was employed to compute the flame speed for each mixture variation. The baseline flame speed for the stoichiometric CH_4-air mixture was found to be 38.4 cm/s. As N_2O was incrementally introduced by replacing a portion of the air, a clear decreasing trend in flame speed was observed. With the addition of 5% N_2O, the flame speed dropped to 33.0 cm/s. Increasing the N_2O concentration to 10% further reduced the flame speed to 29.0 cm/s. When 15% N_2O was added, the flame speed declined to 27.5 cm/s, and at 20% N_2O, the lowest flame speed of 27.0 cm/s was recorded the flame speed result was shown in **Figure 4**.

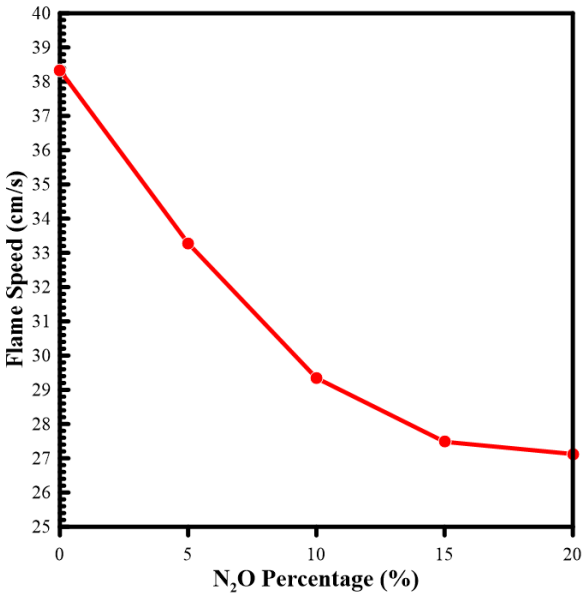

Figure 4. Laminar flame speed of different N_2O concentrations

This reduction in flame speed is primarily attributed to the replacement of air with N_2O, which effectively decreases the mole fraction of O_2 in the reactant mixture. Since molecular oxygen is the primary oxidizer in methane combustion, a reduction in its concentration leads to a slower overall reaction rate. Consequently, this slower reaction rate results in a lower flame propagation speed. Although N_2O can act as an oxidizer through thermal decomposition, under the conditions of this study, its contribution was insufficient to compensate for the loss of O_2, leading to a net decrease in flame speed. This is supported by the study from [32], where the addition of N_2O as a replacement for O_2 in the premixed mixture decreases the burning velocity, thereby inhibiting the flame.

Although N_2O is a strong oxidizer, it requires high temperatures to decompose into N_2 and reactive atomic oxygen (O), which can then participate in radical chain reactions, N_2O is thermally activated and only becomes significant at elevated flame temperatures. As a result, in the initial flame region especially in premixed combustion scenarios, the contribution of N_2O as an oxidizer is limited compared to molecular O_2. Thus, despite its oxidizing potential, the replacement of air with N_2O leads to a net reduction in flame speed, due to both the lower O_2 availability and the dilution effect introduced by additional inert N_2 from N_2O decomposition.

After obtaining the flame speed results, a further analysis was conducted to evaluate the mole fractions of combustion products, particularly reactive radicals, for CH_4-air premixed flames with varying N_2O concentrations ranging from 5% to 20%. As illustrated in **Figure 5a**, the OH radical concentration shows distinct behavior depending on the N_2O content. For the mixture with 15% N_2O, the OH mole fraction reaches its peak at the flame front, indicating more intense radical formation at the reaction zone under this condition. In contrast, in the post-flame region, the flame with 20% N_2O exhibits the highest OH mole fraction among all cases. This phenomenon can be explained by the thermal decomposition behavior of N_2O. Nitrous oxide acts as a thermal oxidizer, decomposing at high temperatures according to the reaction in Eq. (7).

$$N_2O \rightarrow N_2 + O \tag{7}$$

The atomic oxygen (O) produced then participates in radical reactions (Eq. (8) and Eq. (9)), such as:

$$O + H_2 \rightarrow OH + H \tag{8}$$

or

$$O + CH_3 \rightarrow OH + CH_2 \tag{9}$$

At higher N_2O concentrations, such as 20%, more thermal energy is required to trigger this decomposition, delaying the formation of OH radicals into the post-flame zone. As a result, the OH concentration is distributed further downstream, and its peak shifts away from the flame front, resulting in a higher OH abundance after the main combustion zone.

Figure 5b presents the simulated mole fraction profiles of nitric oxide (NO) formed during the combustion process. As N_2O is introduced into the CH_4-air flame, a significant increase in NO formation is observed, particularly in the post-flame region. This trend is expected, since N_2O serves as a source of nitrogen and oxygen, both of which contribute to NO formation through thermal and prompt NO mechanisms. Among all the cases, the mixture with 20% N_2O exhibits the highest NO mole fraction. The elevated NO production in this case is primarily attributed to the increased availability of nitrogen-containing species from N_2O decomposition and the higher

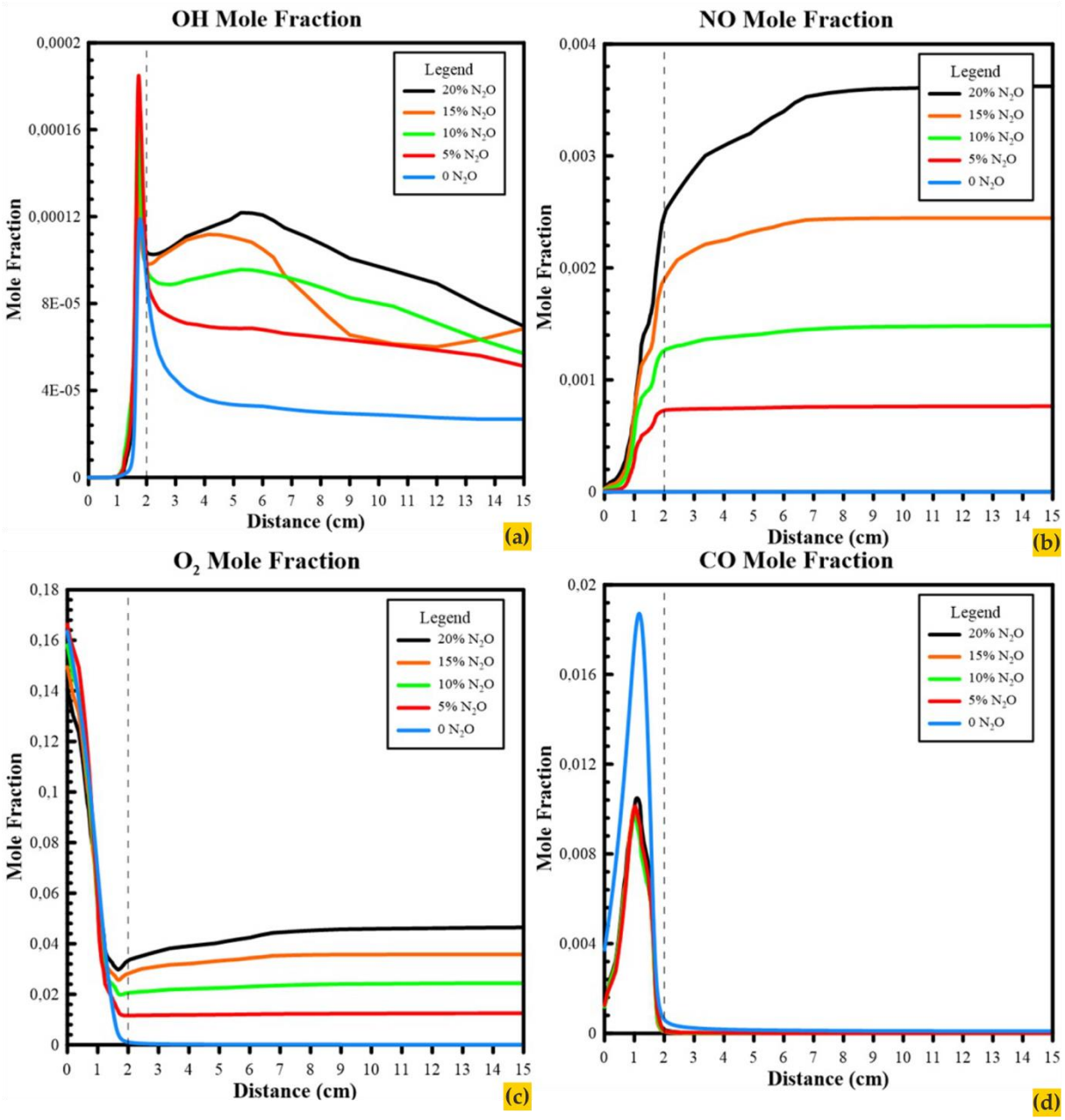

Figure 5. The selected mole fraction results

flame temperatures that enhance thermal NO formation.

Figure 5c shows the mole fraction profiles of molecular oxygen (O_2) across the flame. As expected, O_2 is rapidly consumed at the flame front due to the oxidation reactions with CH_4. However, an interesting trend is observed in the post-flame region: as the concentration of N_2O increases, the mole fraction of O_2 in the post-flame zone also increases. This phenomenon can be attributed to the thermal decomposition of N_2O at high temperatures. According to Eq. (7), N_2O breaks down into nitrogen (N_2) and molecular oxygen (O_2) in the high-temperature environment of the post-flame region. As more N_2O is added to the mixture, a higher amount of O_2 is released through this decomposition pathway, leading to a noticeable increase in O_2 concentration after the main combustion zone. This secondary release of O_2 does not significantly affect the flame front, where combustion is primarily driven by the O_2 supplied from the initial CH_4-air mixture.

Figure 5d presents the mole fraction profiles of carbon monoxide (CO) for each N_2O concentration. Based on the simulation results, both the stoichiometric CH_4-air flame (without N_2O) and the case with 5% N_2O still exhibit noticeable levels of CO in the post-flame region. In

contrast, at higher N_2O concentrations specifically at 10%, 15%, and 20%—the CO mole fraction in the post-flame zone tends to approach zero.

This trend suggests that the addition of N_2O enhances the oxidation of CO-to-CO_2, resulting in more complete combustion. The key factor behind this behavior is the increased availability of reactive oxygen species, particularly atomic oxygen (O), which is generated through the thermal decomposition of N_2O at high temperatures. The released atomic oxygen promotes the following oxidation reaction in Eq. (10).

$$O + CH_3 \rightarrow OH + CH_2 \quad (10)$$

As N_2O concentration increases, more oxygen becomes available in the post-flame region, accelerating the conversion of CO into CO_2 and thereby reducing CO emissions. This effect indicates that N_2O addition to a stoichiometric CH_4-air flame can improve post-flame oxidation efficiency, contributing to cleaner combustion with lower CO residue.

An integrated analysis of mole fractions and net reaction rates was conducted to identify the dominant reaction pathways and evaluate the impact of N_2O addition in the combustion process. The primary focus of this analysis is directed toward reactions involving N_2O, aiming to understand its contribution to flame dynamics and potential changes in emissions. Selected net reaction rates from the reaction mechanism involving dinitrogen oxide (N_2O) in the methane–air combustion system with N_2O addition are presented. These reactions were selected based on their significant contribution to the formation and consumption of key species such as NO, O_2, OH, and other radicals. The selected reactions were not arbitrarily taken from GRI 3.0. But we chose based on their dominant role and formation on radical formation and NO consumption which is taken from CHEMKIN simulation, is shown in **Table 2**.

Reaction 182 is the primary pathway that directly produces NO through the interaction between N_2O and atomic oxygen, making it highly relevant in NO_x formation. Meanwhile, reaction 181 also involves atomic oxygen as a reactant, but instead yields O_2, which can potentially reduce the concentration of active free radicals and indirectly influence the oxidation rate. Reactions 183 and 184 involve H and OH radicals, both of which play crucial roles in combustion chain reactions. The products of these reactions, such as OH and HO_2, can contribute to the formation of other oxidizing species or support radical regeneration processes. Reaction 185 represents the thermal dissociation of N_2O, which is promoted by the presence of a third body (M), resulting in the formation of N_2 and atomic oxygen. This reaction is endothermic and sensitive to both temperature and system pressure, serving as one of the key pathways for supplying free oxygen atoms for subsequent oxidation reactions. The comparison of net reaction rates for each reaction under varying N_2O compositions is presented in the **Figure 6**.

Based on the results, the case with 20% N_2O exhibits the highest overall net reaction rate among the tested conditions. This indicates that increasing the N_2O concentration enhances the reactivity of the system, particularly in reactions involving nitrogen and oxygen species. The elevated net reaction rate at 20% N_2O suggests a more active role of N_2O in influencing radical formation and promoting pathways that contribute to NO_x production as well as the overall combustion dynamics.

In addition to the one-dimensional simulations performed using CHEMKIN Pro, a computational fluid dynamics (CFD) simulation was also conducted using ANSYS Fluent. **Figure 7** displays the results of the CFD modeling of CH_4-air premixed flames with N_2O replacement. In this study, several representative cases were selected to illustrate the effect of varying N_2O concentrations. Figures (a) through (c) show the flame structure results for N_2O concentrations of 5%, 10%, and 20%, respectively. The temperature

Table 2. Selected reaction pathways

Number of Reaction	Reactant	Product
181	N_2O+O	N_2+O_2
182	N_2O+O	2NO
183	N_2O+H	N_2+OH
184	N_2O+OH	N_2+HO_2
185	N_2O(+M)	N_2+O(+M)

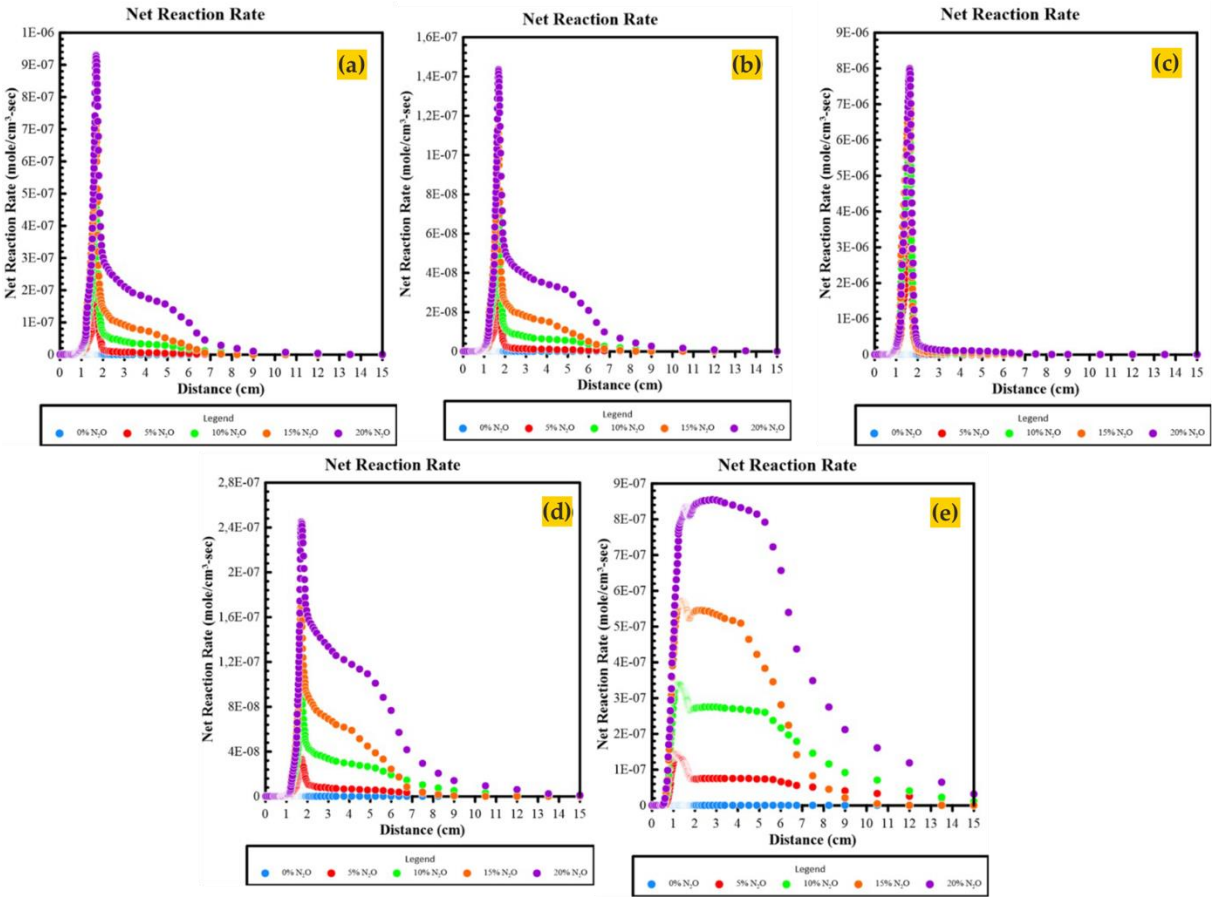

Figure 6. The selected net reaction rate with different N_2O concentration

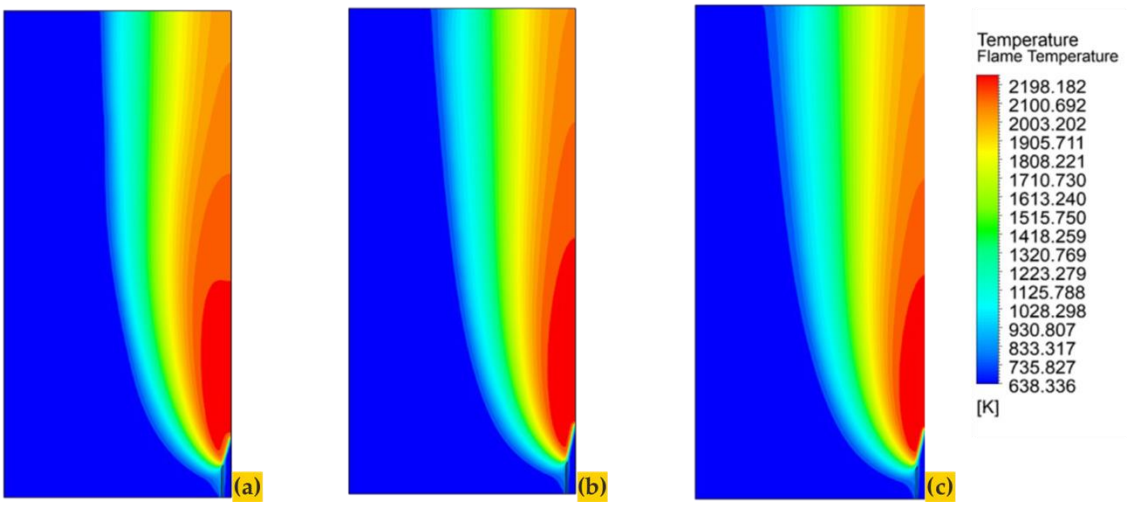

Figure 7. Flame structure of different N_2O concentration at 5% (a), 10% (b), and 20% (c).

distributions from the CFD simulations reveal that the increase in flame temperature with higher N_2O concentrations is relatively moderate. Specifically, in the case of 20% N_2O addition, the temperature in the post-flame region reaches approximately 2200 K. This result is consistent with the adiabatic flame temperature trends obtained from the CHEMKIN simulations, confirming that the inclusion of N_2O has a limited but noticeable effect on raising the overall flame temperature. This agreement between CFD and CHEMKIN results validates the reliability of both approaches and supports the conclusion that N_2O can serve as an additional oxidizer to slightly enhance the thermal characteristics of premixed methane-air combustion.

Figure 8 presents a comparison between the simulated mole fraction distribution of OH radicals and a photographic image of the flame structure. The OH radical profile, obtained from the numerical simulation, is known to represent the high-temperature reaction zone, which correlates closely with the visible flame front observed in the experiment. The comparison shows a strong agreement between the simulation and the actual flame image. Both the simulated OH distribution and the flame photograph highlight the same flame front structure and location, indicating that the simulation accurately captures the flame behavior. This consistency further validates the accuracy of the combustion model and confirms that OH radicals can be used as a reliable indicator for identifying the flame front in premixed methane-air combustion.

3.2. *Experimental Results*

To validate the simulation results, experimental tests were conducted for each N_2O composition. **Figure 9** shows photographic images of the flame structure produced under different conditions. **Figure 9a** displays the CH_4-air premixed flame without N_2O, which exhibits a distinct blue flame front characteristic of clean methane combustion with a relatively high hydrogen-to-carbon ratio [9]. As the concentration of N_2O increases, a noticeable change in flame appearance is observed. The flame color gradually shifts from pure blue to a blue-orange hue, indicating changes in the chemical species and temperature distribution within the flame. According to references [51], [52], [53] indicate that elevated temperatures accelerate soot formation and intensify the emission of orange light. Additionally, the flame front becomes taller with increasing N_2O content, suggesting that the combustion zone extends further downstream. This elongation may be attributed to slower reaction rates or flame stabilization effects due to the modified oxidizer composition, as shown in **Figure 9b** to **Figure 9e**.

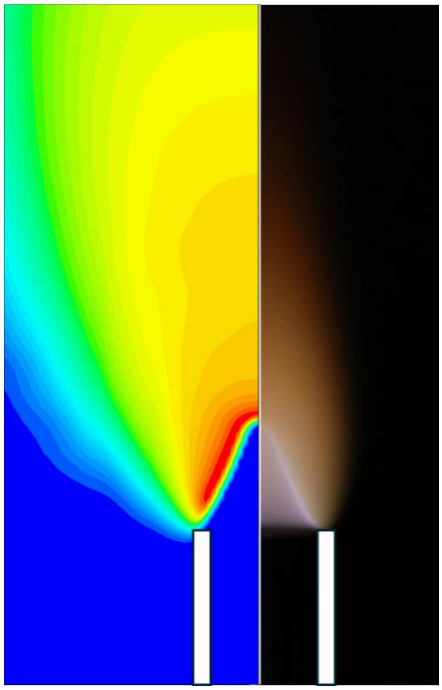

Figure 8. Comparation of OH mole fraction and flame photograph

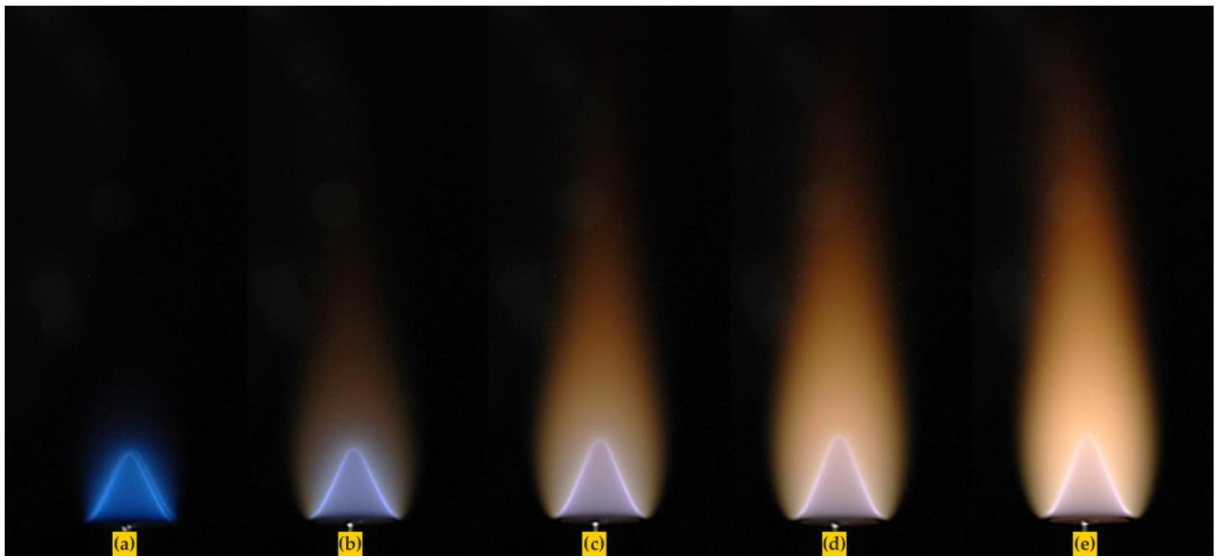

Figure 9. Images of methane-air flames with different N2O concentrations at 0% (a), 5% (b), 10% (c), 15% (d), and 20% (e).

In addition to varying the N_2O concentration from 5% to 20%, an additional case with 25% N_2O replacement was also investigated. However, the resulting flame structure under this condition exhibited signs of instability as shown in **Figure 10**. The flame became less defined and difficult to sustain, indicating poor combustion characteristics. This instability can be attributed to the significant reduction in available O_2 in the oxidation zone due to the replacement of air with N_2O. As the O_2 mole fraction decreases, the primary oxidation reactions between CH_4 and O_2 become less efficient, leading to weakened flame propagation and diminished reaction intensity.

Moreover, the flame speed results obtained from simulation further support this observation. As the concentration of N_2O increases, the laminar flame speed consistently decreases. At 25% N_2O, the flame speed becomes too low to maintain a stable flame under the given operating conditions, highlighting the trade-off between thermal enhancement from N_2O decomposition and the reduction in oxidizing power due to O_2 dilution. These findings emphasize the importance of maintaining an optimal balance between N_2O and O_2 in the reactant mixture to ensure both flame stability and combustion efficiency.

Figure 11 shows how the temperature changes along the flame for different N_2O concentrations (0%, 5%, 10%, 15%, and 20%) in a premixed methane-air combustion system. From the graph, it's clear that adding N_2O affects the flame temperature quite a bit. Without N_2O (just CH_4 and Air), the flame reaches a peak temperature of approximately 1800 K around 30 mm from the burner. When N_2O is added, especially at 10% and 20%, the peak temperature becomes slightly higher, and the high-temperature zone gets wider. The 20% N_2O case has the highest and most stable temperature along a large part of the flame, showing that N_2O boosts the combustion process. This happens because N_2O brings extra oxygen and also takes part in reactions that release more energy. The higher temperature with 20% N_2O also matches the higher net reaction rate, especially in the reaction that forms. Even though the flame gets stronger and hotter with more N_2O, it could also lead to more NO_x emissions due to the higher temperatures and increased radical formation.

Nitrous oxide (N_2O) enhances combustion efficiency and reduces fuel consumption. In comparison to conventional propellant systems, the Nitrous Oxide Fuel Blend Experimental (NOFBX) system demonstrates lower operational costs and reduced fuel storage requirements relative to hydrazine and liquid oxygen (LOX). Furthermore, NOFBX offers improved handling safety, decreased carbon monoxide and carbon dioxide emissions, and is non-toxic. This characteristic of NOFBX NOFBX has strong potential to serve as a future propellant for the aviation industry, supporting both safety and sustainability goals.

Figure 10. Image of methane-air flame with 25% of N_2O concentration

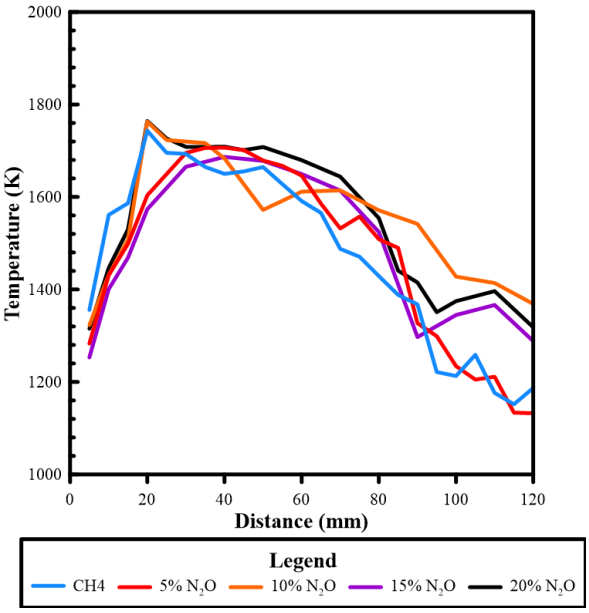

Figure 11. Flame temperature of methane-air flame with different N_2O concentrations

4. Conclusion

Based on the simulation results, replacing O_2 with N_2O in methane-air flames can increase the flame temperature; however, it may also reduce the laminar flame speed due to the decreased O_2 concentration in the reaction zone. In addition, the substitution of N_2O significantly increases NOx formation in the post-flame zone. On the other hand, the use of N_2O leads to a considerable reduction in CO and CO_2 emissions. Experimental results also show that the addition of N_2O at certain concentrations can improve flame stability and raise the flame temperature. However, when the N_2O concentration becomes too high, it can lead to flame instability. The results demonstrate both beneficial and adverse effects of nitrous oxide (N_2O) substitution. N_2O improves thermal performance and decreases carbon-based emissions. However, it also leads to reduced flame speed, increased nitrogen oxides (NOx) emissions, and potential instability at elevated concentrations. Numerical and experimental analyses indicate that N_2O concentrations up to 20% can improve methane flame characteristics.

Author's Declaration

Authors' contributions and responsibilities

The authors made substantial contributions to the conception and design of the study. The authors took responsibility for data analysis, interpretation and discussion of results. The authors read and approved the final manuscript.

Funding

No funding information from the authors.

Availability of data and materials

All data are available from the authors.

Competing interests

The authors declare no competing interest.

Additional information

No additional information from the authors.

References

[1] O. J. Haidn, "Advanced rocket engines," in *Advances on Propulsion Technology for High-Speed Aircraft*, 2008, pp. 6-1-6–40. [Online]. Available: http://www.rto.nato.int

[2] S. M. Davis and N. Yilmaz, "Advances in Hypergolic Propellants: Ignition, Hydrazine, and Hydrogen Peroxide Research," *Advances in Aerospace Engineering*, vol. 2014, pp. 1–9, Sep. 2014, doi: 10.1155/2014/729313.

[3] V. N. Raibhole and S. N. Sapali, "Simulation and Parametric Analysis of Cryogenic Oxygen Plant for Biomass Gasification," *Mechanical Engineering Research*, vol. 2, no. 2, Nov. 2012, doi: 10.5539/mer.v2n2p97.

[4] L. . Hastings, D. . Plachta, L. Salerno, and P. Kittel, "An overview of NASA efforts on zero boiloff storage of cryogenic propellants," *Cryogenics*, vol. 41, no. 11–12, pp. 833–839, Nov. 2001, doi: 10.1016/S0011-2275(01)00176-X.

[5] U. Gotzig, "Challenges and economic benefits of green propellants for satellite propulsion," in *7th European Conference for Aeronautics and Space Sciences (EUCASS)*, 2017.

[6] R. Amrousse, T. Katsumi, N. Azuma, K. Hatai, H. Ikeda, and K. Hon, "Development of green propellants for future space applications," *Science and Technology of Energetic Materials*, vol. 77, no. 5–6, pp. 105–110, 2016.

[7] A. S. Gohardani *et al.*, "Green space propulsion: Opportunities and prospects," *Progress in Aerospace Sciences*, vol. 71, pp. 128–149, Nov. 2014, doi: 10.1016/j.paerosci.2014.08.001.

[8] Y.-H. Li, A. Purwanto, and B.-C. Chuang, "Micro-Explosion mechanism of iron hybrid Methane-Air premixed flames," *Fuel*, vol. 325, p. 124841, Oct. 2022, doi: 10.1016/j.fuel.2022.124841.

[9] Y.-H. Li, S. Pangestu, A. Purwanto, and C.-T. Chen, "Synergetic combustion behavior of aluminum and coal addition in hybrid iron-methane-air premixed flames," *Combustion and Flame*, vol. 228, pp. 364–374, Jun. 2021, doi: 10.1016/j.combustflame.2021.02.013.

[10] L. Werling, M. Haßler, P. Bätz, H. Ciezki, and S. Schlechtriem, "Experimental performance analysis (c∗ & c∗ efficiency) of a premixed green propellant consisting of N2O and C2H4," in *53rd AIAA/SAE/ASEE Joint Propulsion Conference*, 2017. doi: 10.2514/6.2017-5069.

[11] L. Werling *et al.*, "Mono- and Bipropellants Based on Nitrous Oxide and Fuels: State of the Art, Recent Developments in Academia

and Industry, and a Special Focus on DLR's Activities," in *Recent Advancements in Green Propulsion*, 2024, pp. 161–186. doi: 10.1007/978-3-031-62574-9_6.

[12] C. Carmicino, F. Scaramuzzino, and A. Russo Sorge, "Trade-off between paraffin-based and aluminium-loaded HTPB fuels to improve performance of hybrid rocket fed with N2O," *Aerospace Science and Technology*, vol. 37, pp. 81–92, Aug. 2014, doi: 10.1016/j.ast.2014.05.010.

[13] F. Shan, L. Hou, and Y. Piao, "Combustion performance and scale effect from N2O/HTPB hybrid rocket motor simulations," *Acta Astronautica*, vol. 85, pp. 1–11, Apr. 2013, doi: 10.1016/j.actaastro.2012.12.013.

[14] G. Cai, W. Sun, J. Fang, M. Li, Y. Cong, and Z. Yang, "Design and performance characterization of a sub-Newton N2O monopropellant thruster," *Aerospace Science and Technology*, vol. 23, no. 1, pp. 439–451, Dec. 2012, doi: 10.1016/j.ast.2011.10.003.

[15] M. Galle, D. . Agar, and O. Watzenberger, "Thermal N2O decomposition in regenerative heat exchanger reactors," *Chemical Engineering Science*, vol. 56, no. 4, pp. 1587–1595, Feb. 2001, doi: 10.1016/S0009-2509(00)00386-9.

[16] G. Dai *et al.*, "Experimental and kinetic study of N2O thermal decomposition in pressurized oxy-combustion," *Fuel*, vol. 346, p. 128323, Aug. 2023, doi: 10.1016/j.fuel.2023.128323.

[17] C.-H. Chen and Y.-H. Li, "Role of N2O and equivalence ratio on NOx formation of methane/nitrous oxide premixed flames," *Combustion and Flame*, vol. 223, pp. 42–54, Jan. 2021, doi: 10.1016/j.combustflame.2020.10.002.

[18] S. Wang, Z. Wang, A. M. Elbaz, and W. L. Roberts, "Experimental and kinetic studies on laminar burning velocity of NH3/N2O/N2 and CH4/N2O/N2 mixtures under sub-atmospheric and elevated pressures," *Fuel*, vol. 391, p. 134832, Jul. 2025, doi: 10.1016/j.fuel.2025.134832.

[19] B. Nawaz *et al.*, "Combustion characteristics and emissions of nitrogen oxides (NO, NO2, N2O) from spherically expanding laminar flames of ammonia–hydrogen blends," *International Journal of Hydrogen Energy*, vol. 65, pp. 164–176, May 2024, doi: 10.1016/j.ijhydene.2024.03.366.

[20] L.-Q. Wang, D.-G. Chen, and H.-H. Ma, "Propagating characteristics of spherical flames in H2-N2O mixtures," *Process Safety and Environmental Protection*, vol. 175, pp. 575–584, Jul. 2023, doi: 10.1016/j.psep.2023.05.076.

[21] M. Rieth, A. Gruber, and J. H. Chen, "A direct numerical simulation study on NO and N_2O formation in turbulent premixed ammonia/hydrogen/nitrogen-air flames," *Proceedings of the Combustion Institute*, vol. 39, no. 2, pp. 2279–2288, 2023, doi: 10.1016/j.proci.2022.07.266.

[22] M. Mitu, V. Giurcan, C. Movileanu, D. Razus, and D. Oancea, "Propagation of CH4-N2O-N2 Flames in a Closed Spherical Vessel," *Processes*, vol. 9, no. 5, p. 851, May 2021, doi: 10.3390/pr9050851.

[23] L.-Q. Wang, H.-H. Ma, Z.-W. Shen, and J. Pan, "A comparative study of the explosion behaviors of H2 and C2H4 with air, N2O and O2," *Fire Safety Journal*, vol. 119, p. 103260, Jan. 2021, doi: 10.1016/j.firesaf.2020.103260.

[24] M. Lu *et al.*, "Assessment of carbon-free fuel ammonia combustion with low methanol blends in reducing GHG emissions including N2O," *Journal of Cleaner Production*, vol. 463, p. 142755, Jul. 2024, doi: 10.1016/j.jclepro.2024.142755.

[25] Q. Wang *et al.*, "New insights into the NH3/N2O/Ar system: Key steps in N2O evolution," *Proceedings of the Combustion Institute*, vol. 40, no. 1–4, p. 105236, 2024, doi: 10.1016/j.proci.2024.105236.

[26] O. Mathieu, C. M. Grégoire, and E. L. Petersen, "Shock-tube study of the oxidation of ammonia by N2O," *Proceedings of the Combustion Institute*, vol. 40, no. 1–4, p. 105250, 2024, doi: 10.1016/j.proci.2024.105250.

[27] T. Harada *et al.*, "N 2 O Consumption by Thermal Decomposition and Reduction with CH 4 , C 2 H 6 and NH 3," *Combustion Science and Technology*, vol. 197, no. 8, pp. 1655–1671, Jun. 2025, doi: 10.1080/00102202.2023.2289061.

[28] Y. S. Choy, H. S. Zhen, C. W. Leung, and H. B. Li, "Pollutant emission and noise radiation from open and impinging inverse diffusion flames," *Applied Energy*, vol. 91, no. 1, pp. 82–89, Mar. 2012, doi: 10.1016/j.apenergy.2011.09.013.

[29] H.-Y. Shih and J.-R. Hsu, "Computed NO emission characteristics of opposed-jet syngas diffusion flames," *Combustion and Flame*, vol. 159, no. 5, pp. 1851–1863, May 2012, doi: 10.1016/j.combustflame.2011.12.025.

[30] E. K. Dabora, "Effect of NO2 on the ignition delay of CH4-air mixtures," *Combustion and Flame*, vol. 24, pp. 181–184, Feb. 1975, doi: 10.1016/0010-2180(75)90146-7.

[31] M. Yang, Y. Yang, C. Liao, C. Tang, C.-W. Zhou, and Z. Huang, "The auto-ignition boundary of ethylene/nitrous oxide as a promising monopropellant," *Combustion and Flame*, vol. 221, pp. 64–73, Nov. 2020, doi: 10.1016/j.combustflame.2020.07.024.

[32] T. Newman-Lehman, R. Grana, K. Seshadri, and F. Williams, "The structure and extinction of nonpremixed methane/nitrous oxide and ethane/nitrous oxide flames," *Proceedings of the Combustion Institute*, vol. 34, no. 2, pp. 2147–2153, 2013, doi: 10.1016/j.proci.2012.05.102.

[33] D. Razus, M. Mitu, V. Giurcan, C. Movileanu, and D. Oancea, "Methane-unconventional oxidant flames. Laminar burning velocities of nitrogen-diluted methane–N 2 O mixtures," *Process Safety and Environmental Protection*, vol. 114, pp. 240–250, Feb. 2018, doi: 10.1016/j.psep.2017.12.026.

[34] R. J. Kee, F. M. Rupley, E. Meeks, and J. A. Miller, "CHEMKIN-111: A FORTRAN Chemical Kinetics Package for the Analysis of Gas-phase Chemical and Plasma Kinetics," 1999.

[35] O. P. Flames, "PREMIX:A FORTRAN Program for Modeling Steady Laminar One-Dimensional Premixed Flames," 1998.

[36] V. Di Sarli and A. Di Benedetto, "Laminar burning velocity of hydrogen–methane/air premixed flames," *International Journal of Hydrogen Energy*, vol. 32, no. 5, pp. 637–646, Apr. 2007, doi: 10.1016/j.ijhydene.2006.05.016.

[37] G. P. Smith *et al.*, "GRI-Mech 3.0 detailed mechanism," Cerfacs. [Online]. Available: http://combustion.berkeley.edu/gri-mech/

[38] J. G. Yun *et al.*, "Effect of the Oxygen Concentration and Temperature on Thermal Decomposition of N 2 O in an Inert Gas," *ACS Omega*, vol. 6, no. 46, pp. 30983–30988, Nov. 2021, doi: 10.1021/acsomega.1c03365.

[39] V. Giurcan, M. Mitu, C. Movileanu, and D. Razus, "Propagation Characteristics of Stoichiometric Inert-Diluted Methane–N 2 O Flames," *Industrial & Engineering Chemistry Research*, vol. 61, no. 46, pp. 17065–17076, Nov. 2022, doi: 10.1021/acs.iecr.2c03106.

[40] V. Giurcan, M. Mitu, C. Movileanu, D. Razus, and D. Oancea, "Numerical Study of Laminar Flame Propagation in CH4–N2O–N2 at Moderate Pressures and Temperatures," *Combustion, Explosion, and Shock Waves*, vol. 58, no. 1, pp. 22–33, Feb. 2022, doi: 10.1134/S0010508222010038.

[41] H. Saputro, L. Fitriana, A. Purwanto, F. A. Munir, and W.-C. Wang, "A Development of Meso-Scale Vortex Combustion for a Micro Power Generator Based on a Thermoelectric Generator," *Fluids*, vol. 7, no. 12, p. 386, Dec. 2022, doi: 10.3390/fluids7120386.

[42] H. Saputro, L. Fitriana, A. Purwanto, R. Muslim, F. A. Munir, and W.-C. Wang, "Double chamber meso scale vortex combustor for micro scale electric generator based on thermo electric generator," *Energy Reports*, vol. 9, pp. 5015–5030, Dec. 2023, doi: 10.1016/j.egyr.2023.04.010.

[43] Y.-H. Li, P.-H. Lin, W.-Y. Tsai, and J. Lasek, "Comparison of O2-enriched and N2O oxidizers on dual-flame structure and entropy generation," *Case Studies in Thermal Engineering*, vol. 73, p. 106485, Sep. 2025, doi: 10.1016/j.csite.2025.106485.

[44] L. Fitriana, A. Purwanto, F. A. Munir, W.-C. Wang, and H. Saputro, "Optimization of cylindrical stepped micro-combustors for enhanced thermoelectric power generation: A comprehensive numerical and experimental study on wire mesh positioning and material selection," *e-Prime - Advances in Electrical Engineering, Electronics and Energy*, vol. 13, p. 101065, Sep. 2025, doi: 10.1016/j.prime.2025.101065.

[45] ANSYS, *ANSYS Fluent Theory Guide Release 15*. 2013.

[46] ANSYS, *ANSYS Meshing User's Guide*. 2013.

[47] F. Berni, G. Cicalese, M. Borghi, and S. Fontanesi, "Towards grid-independent 3D-CFD wall-function-based heat transfer models for complex industrial flows with focus on in-cylinder simulations," *Applied Thermal Engineering*, vol. 190, p. 116838, May 2021, doi: 10.1016/j.applthermaleng.2021.116838.

[48] A. Seeni, P. Rajendran, and H. Mamat, "A CFD mesh independent solution technique for low reynolds number propeller," *CFD Letters*, vol. 11, no. 10, pp. 15–30, 2019.

[49] Y. A. Cengel, *Heat and mass transfer: a practical approach*. McGraw-Hill, 2007.

[50] B. A. Rabee, "The effect of inverse diffusion flame burner-diameter on flame characteristics and emissions," *Energy*, vol. 160, pp. 1201–1207, Oct. 2018, doi: 10.1016/j.energy.2018.07.061.

[51] Z. Su, Y. Ying, C. Chen, R. Zhao, X. Zhao, and D. Liu, "Effects of diluent gases on sooting transition process in ethylene counterflow diffusion flames," *RSC Advances*, vol. 12, no. 28, pp. 18181–18196, 2022, doi: 10.1039/D2RA02409H.

[52] S. Algoraini, Z. Sun, B. B. Dally, and Z. T. Alwahabi, "Low-pressure ethylene/air laminar premixed flames: characterisations and soot diagnostics," *Applied Physics B*, vol. 129, no. 2, p. 28, Feb. 2023, doi: 10.1007/s00340-023-07975-3.

[53] S. Walther, T. Li, D. Geyer, A. Dreizler, and B. Böhm, "Soot and Flame Structures in Turbulent Partially Premixed Jet Flames of Pre-Evaporated Diesel Surrogates with Admixture of OMEn," *Fluids*, vol. 9, no. 9, p. 210, Sep. 2024, doi: 10.3390/fluids9090210.